αvβ3-integrin regulates PD-L1 expression and is involved in cancer immune evasion

Andrea Vannini[a], Valerio Leoni[a], Catia Barboni[b], Mara Sanapo[b], Anna Zaghini[b], Paolo Malatesta[c,d], Gabriella Campadelli-Fiume[a,1], and Tatiana Gianni[a]

[a]Department of Experimental, Diagnostic and Specialty Medicine, University of Bologna, 40126 Bologna, Italy; [b]Department of Veterinary Medical Sciences, University of Bologna, 40064 Bologna, Italy; [c]Department of Experimental Medicine, University of Genova, 16132 Genova, Italy; and [d]Ospedale Policlinico San Martino, Istituto di Ricovero e Cura a Carattere Scientifico (IRCCS), 16132 Genova, Italy

Edited by Tasuku Honjo, Graduate School of Medicine, Kyoto University, Kyoto, Japan, and approved August 22, 2019 (received for review February 1, 2019)

Tumors utilize a number of effective strategies, including the programmed death 1/PD ligand 1 (PD-1/PD-L1) axis, to evade immune-mediated control of their growth. PD-L1 expression is mainly induced by IFN receptor signaling or constitutively induced. Integrins are an abundantly expressed class of proteins which play multiple deleterious roles in cancer and exert proangiogenic and prosurvival activities. We asked whether αvβ3-integrin positively regulates PD-L1 expression and the anticancer immune response. We report that αvβ3-integrin regulated constitutive and IFN-induced PD-L1 expression in human and murine cancerous and noncancerous cells. αvβ3-integrin targeted STAT1 through its signaling C tail. The implantation of β3-integrin–depleted tumor cells led to a dramatic decrease in the growth of primary tumors, which exhibited reduced PD-L1 expression and became immunologically hot, with increased IFNγ content and CD8+ cell infiltration. In addition, the implantation of β3-integrin–depleted tumors elicited an abscopal immunotherapeutic effect measured as protection from the challenge tumor and durable splenocyte and serum reactivity to B16 cell antigens. These modifications to the immunosuppressive microenvironment primed cells for checkpoint (CP) blockade. When combined with anti–PD-1, β3-integrin depletion led to durable therapy and elicited an abscopal immunotherapeutic effect. We conclude that in addition to its previously known roles, αvβ3-integrin serves as a critical component of the cancer immune evasion strategy and can be an effective immunotherapy target.

αvβ3-integrin | PD-L1 expression | cancer immunotherapy | combination therapy | immune evasion

The programmed death 1/PD ligand 1 (PD-1/PD-L1) axis is a major arm of the immune system that regulates the immune response to cancer and is the subject of intense study of cancer immunotherapy (1, 2). PD-L1 is expressed in cells of different lineages, including immune and tumor cells (2, 3). PD-L1 expression may be constitutive or regulated by a number of signaling pathways that activate transcription factors, by posttranscriptional events through specific microRNAs and by epigenetic factors. Inducible PD-L1 expression is triggered mainly by interferon γ (IFNγ) through IFN receptor (IFNR) signaling or by the binding of other cytokines, including IFNα/β, and by Toll-like receptors (TLRs) 4 (3–8). Additional signaling pathways and factors that regulate PD-L1 expression are those of mitogen-activated protein kinase (MAPK)/c-Jun, phosphoinositide 3-kinase (PI3K)/AKT, hypoxia, and the transcription factors signal transducer and activator of transcription 3 (STAT3) and nuclear factor κ-light-chain enhancer of activated B cells (NF-κB) (6). PD-L1 expression is a negative prognostic factor in cancer (2, 9–11). Immunotherapy based on monoclonal antibodies that disrupt the PD-1/PD-L1 axis (checkpoint [CP] inhibitors; CPIs) is active against only certain groups of cancers. Among patients with these susceptible cancers, only a fraction of patients respond to CPIs (2). In patients who respond to CPIs, resistance that frequently maps to IFNR signaling develops (12, 13). CPI therapy is accompanied by adverse effects.

Integrins are multifunctional αβ-heterodimers that regulate cell–cell and cell–matrix interactions through signaling and play numerous critical roles, including the regulation of the cell cycle and proliferation, in part via cooperation with growth factor receptors (14–17). Abundantly expressed in tumors, integrins, including αvβ3-integrin (herein αvβ3-int), contribute to the acquisition of a metastatic phenotype and stemness (18–20). αvβ3-int in endothelial cells contributes to neoangiogenesis (15, 21). Cilengitide (herein *cln*) is an approved αvβ3-antagonist with antiangiogenic activity against certain tumors (15); however, its efficacy in humans has been debated (22). Since *cln* was administered as an antiangiogenic compound in earlier work, there has been no investigation of its effect on PD-L1 expression and sensitivity to CPIs. Integrins frequently cooperate with receptors, such as epidermal growth factor receptor (EGFR), boosting their tyrosine kinase activity (23, 24). We and others discovered that αvβ3-int contributes greatly to the innate response to viral and bacterial pathogens (25, 26); the molecular basis for this contribution is the cooperation of αvβ3-int with specific TLRs, boosting their signaling activity (27). αvβ3-int also drives the innate tumor response (28).

In this work, we show that αvβ3-int cooperates with and regulates IFNα/βR and IFNγR signaling in human cancerous and noncancerous cells by targeting STAT1 and positively regulates PD-L1 expression. A decrease in IFNR signaling and PD-L1 expression

Significance

The PD-1/PD-L1 axis is a master player in the tumor immune evasion strategy. Checkpoint inhibitors, including anti–PD-1/PD-L1, are revolutionizing cancer immunotherapy. There is intense interest in dissecting their regulation and improving their application, mainly by combination therapies. The significance of the current findings is 2-fold. Our results suggest αvβ3-integrin as a critical regulator of PD-L1 expression and a key component of the tumor immune evasion machinery. Indeed, αvβ3-integrin depletion impairs tumor growth and elicits immunotherapeutic protection. Second, αvβ3-integrin blockade primes tumors for anti–PD-1 therapy and induces durable anticancer immune protection when combined with anti–PD-1 therapy. αvβ3-integrin is a readily druggable target that adds to the list of molecules suitable for combinatorial cancer immunotherapy.

Author contributions: A.V., G.C.F., and T.G. designed research; A.V., V.L., C.B., M.S., and T.G. performed research; A.V., V.L., A.Z., and G.C.F. designed animal studies; P.M. contributed new reagents/analytic tools; A.V., V.L., C.B., M.S., A.Z., P.M., G.C.F., and T.G. analyzed data; and A.V., G.C.F., and T.G. wrote the paper.

The authors declare no conflict of interest.

This article is a PNAS Direct Submission.

[1]To whom correspondence may be addressed. Email: gabriella.campadelli@unibo.it.

This article contains supporting information online at www.pnas.org/lookup/suppl/doi:10.1073/pnas.1901931116/-/DCSupplemental.

First published September 16, 2019.

upon β3-int depletion or agonistic peptide inhibition was also observed in murine melanoma cells, not only in vitro but also in vivo. The implantation of β3-int–depleted tumor cells dramatically decreased primary tumor growth; protected against the growth of contralateral challenge tumors, which were characterized by immune cell infiltration and increased PD-L1 expression; and played a role in systemic antitumor immune responses. The combination of β3-int depletion and anti–PD-1 led to highly effective immunotherapy.

Results

αvβ3-Integrin Regulates IFNR Signaling in Cancerous and Noncancerous Cells. To ascertain whether αvβ3-int regulates IFNR signaling, we blocked αvβ3-int through either depletion or the specific inhibitor *cln* (29). To deplete αvβ3-int, epithelial HaCaT and neuronal SK-N-SH cells were transduced with lentivirus encoding β3-int short hairpin (sh)RNA (named shβ3). The extent of silencing was greater than 85% (Fig. 1*A* and *SI Appendix*, Fig. S1*A*). HaCaT and SK-N-SH cells were or were not exposed to IFNα, β, and γ. The extent of the phosphorylation of molecules involved in IFNR signaling in HaCaT cells is shown in Fig. 1 *B* and *C*, and that in SK-N-SH cells in *SI Appendix*, Fig. S1 *B* and *C*. β3-int depletion, or its blockade with *cln*, strongly diminished IFNα-, β-, and γ-induced STAT1 and mitogen-activated protein kinase kinase 1/2 (MEK1/2) phosphorylation, and exerted a much lesser effect on Janus kinase 1 (JAK1) phosphorylation. Since the effects of β3-int depletion or *cln* blockade were almost indistinguishable, a panel of cancer cell lines derived from ovarian cancer (SK-OV-3), breast cancers (SK-BR-3, MDA-MB-453), hepatoma (HT29), and glioblastoma (U251) were treated with *cln* and exposed to IFNα, β, or γ. In all cell lines tested, the IFN-induced phosphorylation of STAT1 and MEK1/2 was dramatically decreased, whereas that of JAK1 was scarcely modified (Fig. 1 *D* and *E* and *SI Appendix*, Fig. S1 *D–F*). With the exception of MEK1/2 phosphorylation in HaCaT cells, the tested molecules exhibited no detectable or very little phosphorylation in the absence of IFN. Hence, the effect of β3-int depletion on basal activation could not be tested. Altogether, these results indicate that αvβ3-int block inhibited the IFNR pathway, mostly at the level of STAT1 and downstream. The decrease in inducible MEK1/2 phosphorylation may reflect in part a requirement for the MAPK cascade in IFN-stimulated gene expression (30). The inhibition of IFNR signaling was observed in noncancerous and cancerous cells from different tumors.

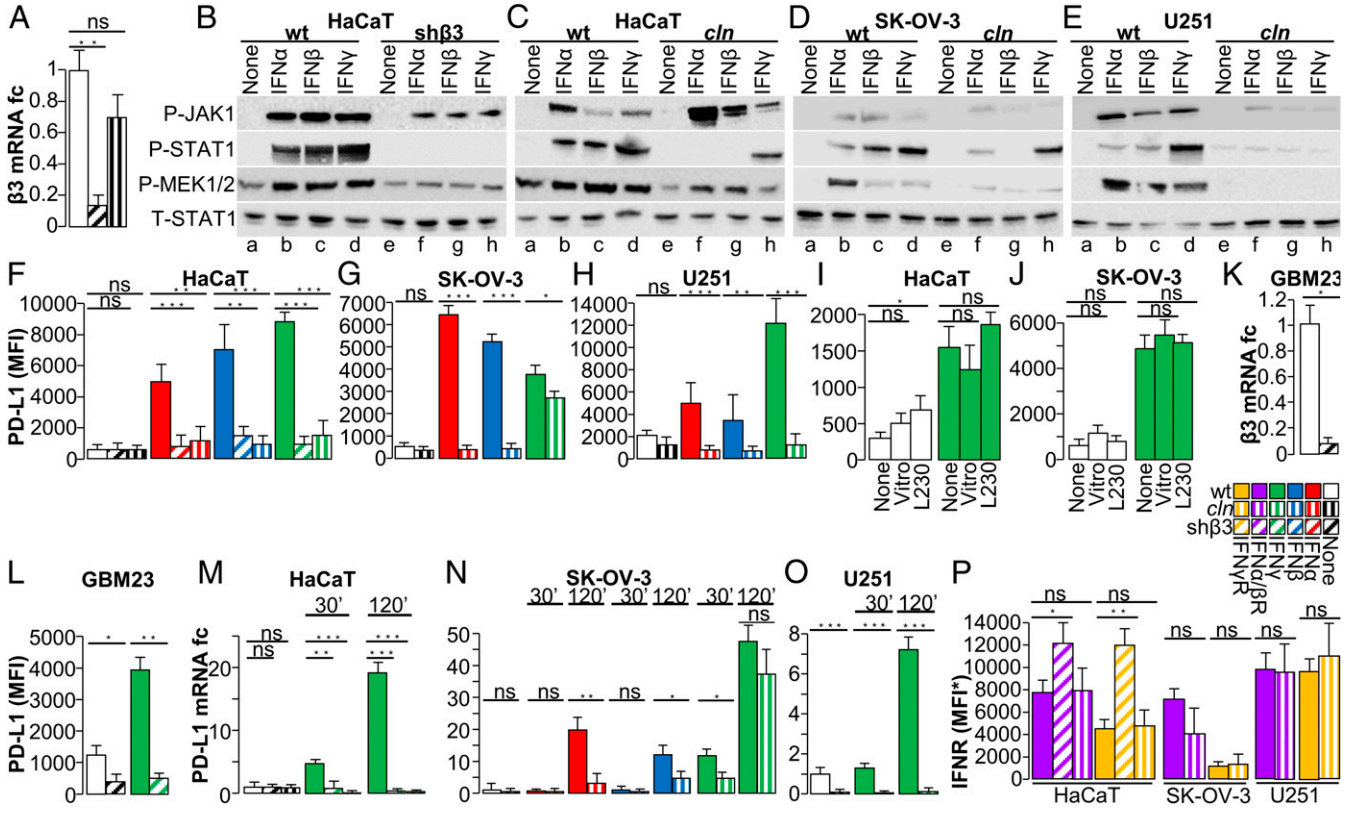

Fig. 1. β3-integrin block hinders the signaling cascade of IFNα/β- and γ-receptors and decreases PD-L1 expression. (*A*) Expression of β3-int in HaCaT cells, depleted of β3-int, or treated with *cln*. fc, fold change. (*B–E*) Effect of β3-int block on IFNα/β- and γ-receptor signaling. WT cells, cells silenced for β3-int (shβ3), or *cln*-pretreated cells were unexposed (None) (lanes a and e) or exposed to IFNα (lanes b and f), IFNβ (lanes c and g), or IFNγ (lanes d and h) for 10 min (for P-JAK1) and 30 min (for the other proteins). P-JAK1, P-STAT1, P-MEK1/2, or the total amount of STAT1 (T-STAT1) was detected with specific antibodies. (*F–H*) Effect of β3-int block on PD-L1 expression. WT, shβ3, or *cln*-treated cells were exposed to IFNα, IFNβ, or IFNγ for 48 h and reacted with an antibody to human PD-L1-APC. Mean fluorescence intensity (MFI) of gated cells was quantified by flow cytometry. (*I* and *J*) Effect of αvβ3-int activation on PD-L1 expression. HaCaT (*I*) and SK-OV-3 cells (*J*) were unexposed (None) or exposed to vitronectin or MAb L230 for 24 h and induced with IFNγ 500 (HaCaT) or IFNα 100 IU (SK-OV-3). PD-L1 was quantified as MFI. (*K* and *L*) Effect of β3-int silencing on PD-L1 expression in GBM23 cells stably silenced for β3-int (GBM23shβ3) or mock-silenced (GBM23ctrl). (*K*) Silencing was measured by qRT-PCR at 48 h. (*L*) Reduction in PD-L1 expression (MFI) in β3-int–depleted cells induced with 100 U IFNγ. (*M–O*) Effect of β3-int block on PD-L1 transcription in HaCaT (*M*), SK-OV-3 (*N*), and U251 (*O*) cells, depleted of β3-int (shβ3) or treated with *cln*, and exposed to IFNγ for 30 or 120 min. SK-OV-3 cells were exposed also to IFNα and IFNβ for the same time intervals; amounts of IFNs were 100, 500, or 1,000 IU in SK-OV-3, HaCaT, or U251 cells. (*P*) Expression of IFNα/β- and γ-receptors in HaCaT, SK-OV-3, or U251 cells, depleted of β3-int, or treated with *cln*. Levels of IFNR were expressed as MFI* (MFI values of anti-IFNR–stained samples subtracted of MFI values of isotype controls). In *A* and *F–P*, histograms represent the average of triplicates ±SD. *B–E* are representative images of repeated (triplicate) experiments. Statistical significance was calculated by means of the *t* test (*G*, *H*, *K*, *L*, and *N–P*) or 1-way ANOVA (*A*, *F*, *I*, *J*, *M*, and *P*). $*P < 0.05$, $**P < 0.01$, $***P < 0.001$; ns, nonsignificant.

αvβ3-Int Positively Regulates the IFNα-, IFNβ-, and IFNγ-Inducible Expression of PD-L1. PD-L1 is expressed constitutively, or its expression is induced by IFNα, β, and γ (typically IFNγ), in a cell line-dependent fashion. We asked whether the block in IFNα/βR and IFNγR signaling consequent to β3-int depletion or inhibition altered PD-L1 expression. As shown in Fig. 1 *F–H* and *SI Appendix*, Fig. S1 *G–I*, PD-L1 expression induced by IFNα, β, and γ was dramatically inhibited in HaCaT, SK-OV-3, and U251 cells depleted of β3-int or in additional *cln*-treated cancer cells (*SI Appendix*, Fig. S1 *J–M*). We noted 2 exceptions. *cln* only slightly inhibited IFNγ-induced STAT1 phosphorylation and PD-L1 expression in SK-OV-3 cells (Fig. 1 *D* and *G*). IFNα and β failed to induce PD-L1 expression in MDA-MB-453 cells (*SI Appendix*, Fig. S1*L*). In all cells, the expression of nectin 1, an IFN-independent cell-surface marker, was practically unaffected (*SI Appendix*, Fig. S1 *N–T*). Interestingly, U251 cells were the only cells that exhibited constitutive PD-L1 expression, which was significantly decreased upon *cln* treatment, even in the absence of IFN (Fig. 1*H*). We conclude that αvβ3-int positively regulates constitutive and IFN-induced PD-L1 expression in cancerous and noncancerous cells.

To provide evidence that PD-L1 down-regulation in β3-int–depleted cells could be due to a decrease in IFN signaling—namely P-STAT1 and P-MEK1/2—we incubated wild-type (WT) cells with the P-STAT1 inhibitor fludarabine or the P-MEK1/2 inhibitor U0126. In IFNγ-induced SK-N-SH cells, U0126 decreased MEK1/2 phosphorylation by ∼40% and PD-L1 expression by more than 50% (*SI Appendix*, Fig. S2 *A–C*). No PD-L1 reduction was seen in uninduced cells (*SI Appendix*, Fig. S2 *B* and *C*). In IFNβ-induced HaCaT cells, fludarabine decreased STAT1 phosphorylation by ∼35% and PD-L1 expression by ∼34% (*SI Appendix*, Fig. S2 *D* and *E*). Thus, also in our experimental systems, PD-L1 behaves as a typical IFN-sensitive gene (31).

In cultured cells, αvβ3- and other αv-integrins bind fibronectin, vitronectin, and additional ligands in the matrix and in adjacent cells and are therefore in a partially active state (14). To address the question as to whether the state of integrin affects the constitutive and IFN-induced expression of PD-L1, we maximized αvβ3-int activation by culturing HaCaT and SK-OV-3 cells in the presence of vitronectin or of the highly potent agonist monoclonal antibody (MAb) L230 (25). The phosphorylation of sarcome (SRC) tyrosine-protein kinase and focal adhesion kinase (FAK), 2 molecules downstream of the αvβ3-int pathway, showed αvβ3-int was partially activated in untreated cultures, and that the treatments resulted in further activation (*SI Appendix*, Fig. S2*F*). Under those conditions, cells exhibited small-to-no increase in constitutive and IFNγ-induced PD-L1 expression (Fig. 1 *I* and *J* and *SI Appendix*, Fig. S2 *G* and *H*). The results hint that αvβ3-int was in a partially active state and that no further activation was needed to regulate PD-L1 expression, and suggest that the regulation of PD-L1 expression did not vary whether or not the integrins were activated by exogenous ligands.

The above cell lines have been passaged extensively in culture. To provide clinical significance to our findings, we asked whether αvβ3-int regulates PD-L1 expression in tumor-initiating cells. The human glioblastoma GBM23 cells carry markers of tumor-initiating cells (32). Here, GBM23 cells were depleted of αvβ3-int by shβ3 lentivirus transduction. The extent of β3-int mRNA silencing was greater than 90% (Fig. 1*K*). PD-L1 was up-regulated in response to IFNγ induction in WT cells, but not in the GBM23-shβ3 cells (Fig. 1*L*). The results indicate that the positive regulation exerted by αvβ3-int on IFN-induced PD-L1 expression also occurs in human tumor-initiating cells.

αvβ3-int regulated PD-L1 expression mainly at the transcriptional level (Fig. 1 *M–O*). HaCaT, SK-OV-3, and U251 cells were depleted of β3-int or treated with *cln* and exposed to IFNα, β, or γ. β3-int depletion or blockade abolished constitutive (in U251 cells) and IFN-induced PD-L1 mRNA transcription (Fig. 1 *M–O*). The only exception was observed in SK-OV-3 cells exposed to IFNγ, which was consistent with the results on PD-L1 protein expression.

Next, we depleted β6- or β8-integrin, 2 subunits of the αv family, in SK-N-SH and HT29 cells. The extent of silencing ranged between 85 and 95% (*SI Appendix*, Fig. S2 *I* and *M*). Upon IFNγ induction, both P-STAT1 (*SI Appendix*, Fig. S2 *J* and *N*) and PD-L1 (*SI Appendix*, Fig. S2 *K*, *L*, *O*, and *P*) were mostly unaffected. Hence, the increase in IFNα/βR and IFNγR signaling by αv-integrins was not broadly induced by any αv-integrin but appeared to be specific to some members of the αv family. Interestingly, αvβ8-integrin regulates TGFβ activation in tumor immune cells in a PD-1/PD-L1–independent fashion (33). Thus, different members of the αv family appear to tackle host immunity to cancer by different mechanisms. Of note, the observation that PD-L1 expression is regulated specifically by αvβ3-int together with the finding that *cln* reduced PD-L1 expression in the tested cell lines argues that the inhibitor targeted αvβ3-int, even though its spectrum of action includes other members of the integrin family (34).

The expression of IFNα/βR and IFNγR upon β3-int blockade was moderately affected in HaCaT, SK-OV-3, and U251 (Fig. 1*P*), with minor variations at the mRNA level in all of the tested cells (*SI Appendix*, Fig. S2*Q*). Thus, for the majority of the cell lines employed in this study, the decrease in PD-L1 expression upon β3-int blockade was unlikely to be due to a decrease in IFN receptors. Additionally, of note was the finding that upon IFN exposure, αvβ3-int expression itself did not significantly change (*SI Appendix*, Fig. S2 *R* and *S*).

αvβ3-Int Regulates Additional IFN-Stimulated Genes, IRF7 and SOCS1. We measured the αvβ3-int–mediated regulation of IFN regulatory transcription factor 7 (IRF7). The depletion or *cln* inhibition of β3-int decreased the IFNα-, β-, and γ-induced expression of IRF7 in HaCaT, SK-OV-3, and U251 cells (Fig. 2 *A–C*). Thus, similar to PD-L1, IRF7 was positively regulated by αvβ3-int.

Suppressor of cytokine signaling (SOCS) proteins negatively modulate IFNR signaling at the posttranslational level. They are induced by IFNs and act through a negative feedback mechanism (35). SOCS1 targets STAT1; therefore, we asked whether β3-int blockade modifies SOCS1 expression. HaCaT, SK-OV-3, and U251 cells were depleted of β3-int or treated with *cln* and exposed to IFNs. In all of the cells, IFN-induced SOCS1 expression—at the mRNA and protein levels—was up-regulated or not significantly modified in β3-int–depleted or *cln*-treated cells (Fig. 2 *D–I*). Altogether, αvβ3-int positively regulated IRF7 and PD-L1 expression and negatively regulated SOCS1. How β3-int regulates SOCS1 and the effects of SOCS1 modulation on PD-L1 expression remain to be elucidated.

β3-Int Regulates the IFN Pathway through Its Signaling C Tail. αvβ3-int signaling is mediated through the Y747 and Y759 residues in the β3 C-terminal (C) tail. Once they are phosphorylated, a number of kinases, including FAK/SRC, MAPK, and PI3K/AKT, are recruited or activated. We asked whether STAT1 phosphorylation is decreased when cells are transfected with a β3-int mutant at residues Y747 and Y759 (Fig. 3*A* and *SI Appendix*, Fig. S3*A*). As shown in Fig. 3 *B* and *C* and *SI Appendix*, Fig. S3*B*, P-STAT1, P-MEK1/2, and PD-L1 were dramatically decreased in SK-OV-3 cells expressing mutant β3-int but not in those expressing WT β3-int (Fig. 3*B*, compare lane f with lane d) or those expressing endogenous integrin (Fig. 3*B*, compare lane f with lane b). This indicates that the regulation of IFNR signaling mediated by αvβ3-int involves the β3-int C tail.

In Murine Melanoma Cells, αvβ3-Int Regulates PD-L1 Expression In Vitro and In Vivo, and Its Depletion Inhibits Tumor Growth. Next, we ascertained whether αvβ3-int regulates PD-L1 expression in

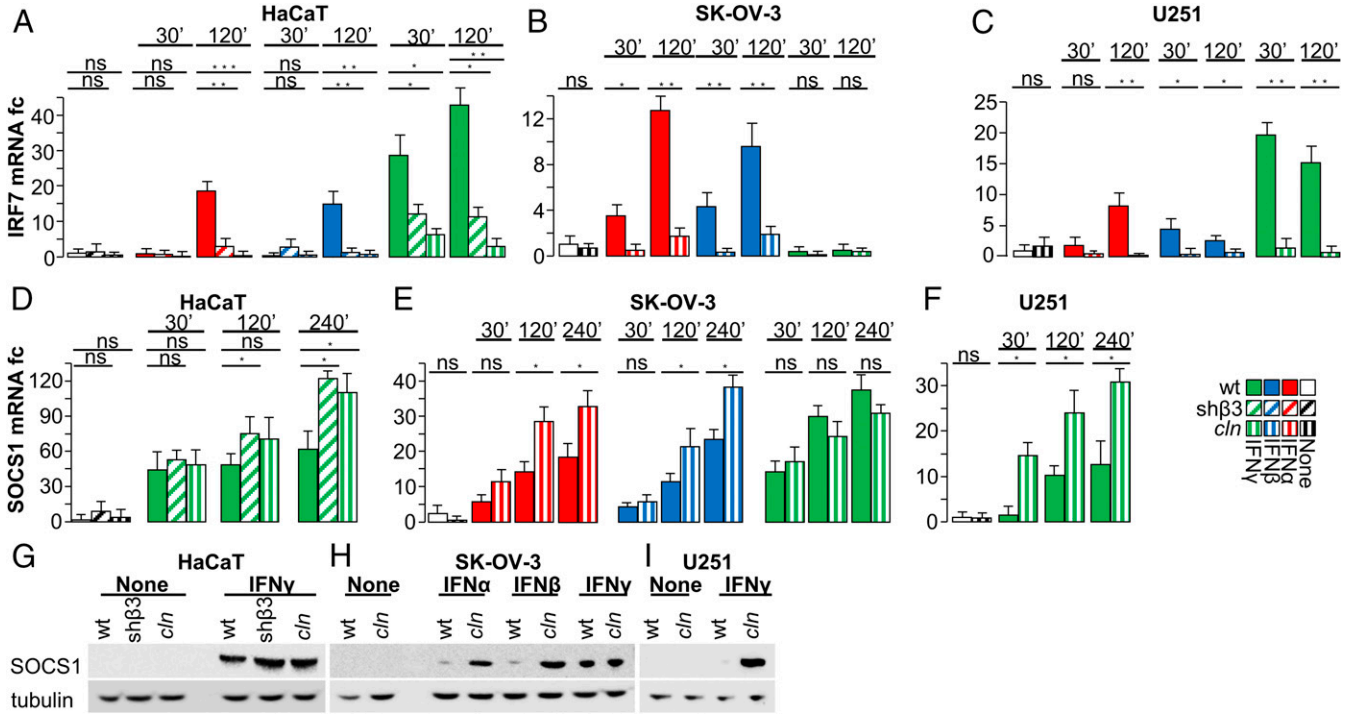

Fig. 2. IFN-regulated genes. (*A–C*) Effect of β3-int block on IRF7. The indicated WT, shβ3, or *cln*-treated cells were exposed to IFNα, IFNβ, or IFNγ for 30 or 120 min, as detailed in Fig. 1. IRF7 mRNA was determined by qRT-PCR. (*D–I*) Effect of β3-int block on SOCS1. Cells were treated as in *A–C*. (*D–F*) SOCS1 mRNA. (*G–I*) WB analysis of SOCS1 and tubulin in the indicated cells. In *A–F*, histograms represent the average of triplicates ±SD. *G–I* are representative images of triplicate experiments. Statistical significance was calculated by means of the *t* test (*B*, *C*, *E*, and *F*) or 1-way ANOVA (*A* and *D*). **P* < 0.05, ***P* < 0.01, ****P* < 0.001; ns, nonsignificant.

murine cancer cells in vitro and in vivo and contributes to tumor immune evasion. Altogether, we employed 2 tumor models, the B16 melanoma cells, syngeneic with C57BL/6 mice and characterized by high constitutive and inducible PD-L1 expression (*SI Appendix*, Fig. S4*A*), and the 4T1 breast cancer cells, syngeneic with BALB/c mice. The murine cancer cells were stably or transiently depleted of β3-int.

Three stably depleted B16 clones (cl 5, cl 19, and cl 38) were generated by shβ3-lentivirus transduction. Control cells received lentiviral control shRNA (ctrl). The 3 shβ3 clones exhibited a reduction in β3-int expression of ∼60 to 75% (Fig. 4*A* and *SI Appendix*, Fig. S4 *A* and *B*), a strong reduction in both constitutive and IFN-induced PD-L1 expression (Fig. 4*B* and *SI Appendix*, Fig. S4 *C* and *D*), as well as a decrease in P-STAT1 (Fig. 4*C*). Thus, in murine B16 cells, constitutive and IFN-dependent PD-L1 expression was also regulated in part by β3-int. Similar to human cells, no significant variation was observed in IFNα/βR and IFNγR in the β3-int–depleted B16 clone (*SI Appendix*, Fig. S4*E*). Variation was also not observed in αvβ3-int cell-surface expression in WT B16 cells upon IFN exposure (*SI Appendix*, Fig. S4*F*).

B16-ctrl and B16-shβ3 clonal cells were implanted in mice to induce tumors. Surprisingly, there was a strong reduction (cl 19 and cl 38) or no tumor growth (cl 5) (Fig. 4 *D–G*). The cumulative number of tumor-free/treated mice was 20/32. When present, tumors were close to the limit of detection at day 23 (Fig. 4*H*). The cumulative reduction in tumor volume was 93%. The tumors in mice from the shβ3 arm exhibited reduced PD-L1 (Fig. 4*I* and *SI Appendix*, Fig. S4*G*), and hence the PD-L1 reduction was maintained in vivo. Further analyses of tumor specimens were halted by a lack of material.

The reduction in growth observed in the shβ3 clones was likely a multifactorial effect, dependent in part on immune dysregulation and PD-L1 decrease (i.e., PD-L1–dependent), and in part PD-L1–independent, i.e., dependent on the integrin-mediated regulation of the cell cycle and proliferation (14–16). To quantify the latter, clone 5, clone 38, and ctrl B16 were implanted in nonobese diabetic/severe combined immunodeficiency (NOD-scid) mice. Fig. 4 *J–M* shows that there was a tendency toward but no statistically significant reduction in tumor growth at day 20. Thus, the reduction in tumor growth in β3-int–depleted clones was ascribed mainly to the PD-L1–dependent immune dysregulation.

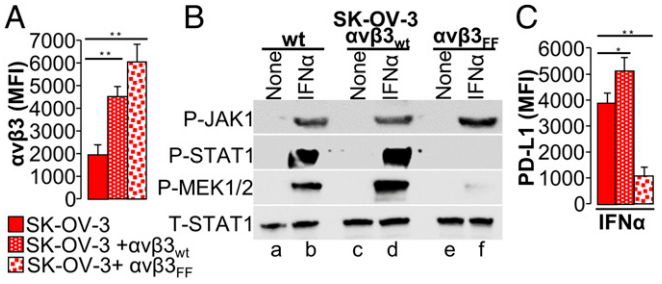

Fig. 3. Mutations in the β3-int C tail hinder the signaling cascade of the IFNα-receptor. (*A*) Extent of β3-int expression in SK-OV-3 cells transiently overexpressing mock plasmid (WT), αv, and WT-β3-int subunits ($\alpha v\beta 3_{wt}$) or αv and mutant $\beta 3_{Y747F,Y759F}$ integrin subunits ($\alpha v\beta 3_{Y747F,Y759F}$). αvβ3-int heterodimer expression was quantified by flow cytometry and expressed as MFI. (*B*) Effect of β3-int C-tail mutant $\beta 3_{Y747F,Y759F}$ on JAK1, STAT1, and MEK1/2 phosphorylation. Total amount of STAT1 (T-STAT1). WT cells, or cells overexpressing αv plus the WT-β3-int subunit ($\alpha v\beta 3_{wt}$) or mutant $\beta 3_{Y747F,759F}$ integrin subunit ($\alpha v\beta 3_{Y747F,Y759F}$), were exposed to IFNα (50 U) for 30 min. (*C*) Effect of β3-int C-tail mutant $\beta 3_{Y747F,Y759F}$ on PD-L1 expression. WT cells, or cells overexpressing αv plus the WT-β3-int subunit ($\alpha v\beta 3_{wt}$) or mutant $\beta 3_{Y747F,Y759F}$ integrin subunit ($\alpha v\beta 3_{Y747F,Y759F}$), were exposed to IFNα (100 IU) for 48 h. PD-L1 expression was detected by flow cytometry, as described in the legend to Fig. 1. In *A* and *C*, histograms represent the average of triplicates ±SD. *B* shows representative images of repeated (triplicate) experiments. Statistical significance was calculated by means of the 1-way ANOVA (*A* and *C*). **P* < 0.05, ***P* < 0.01.

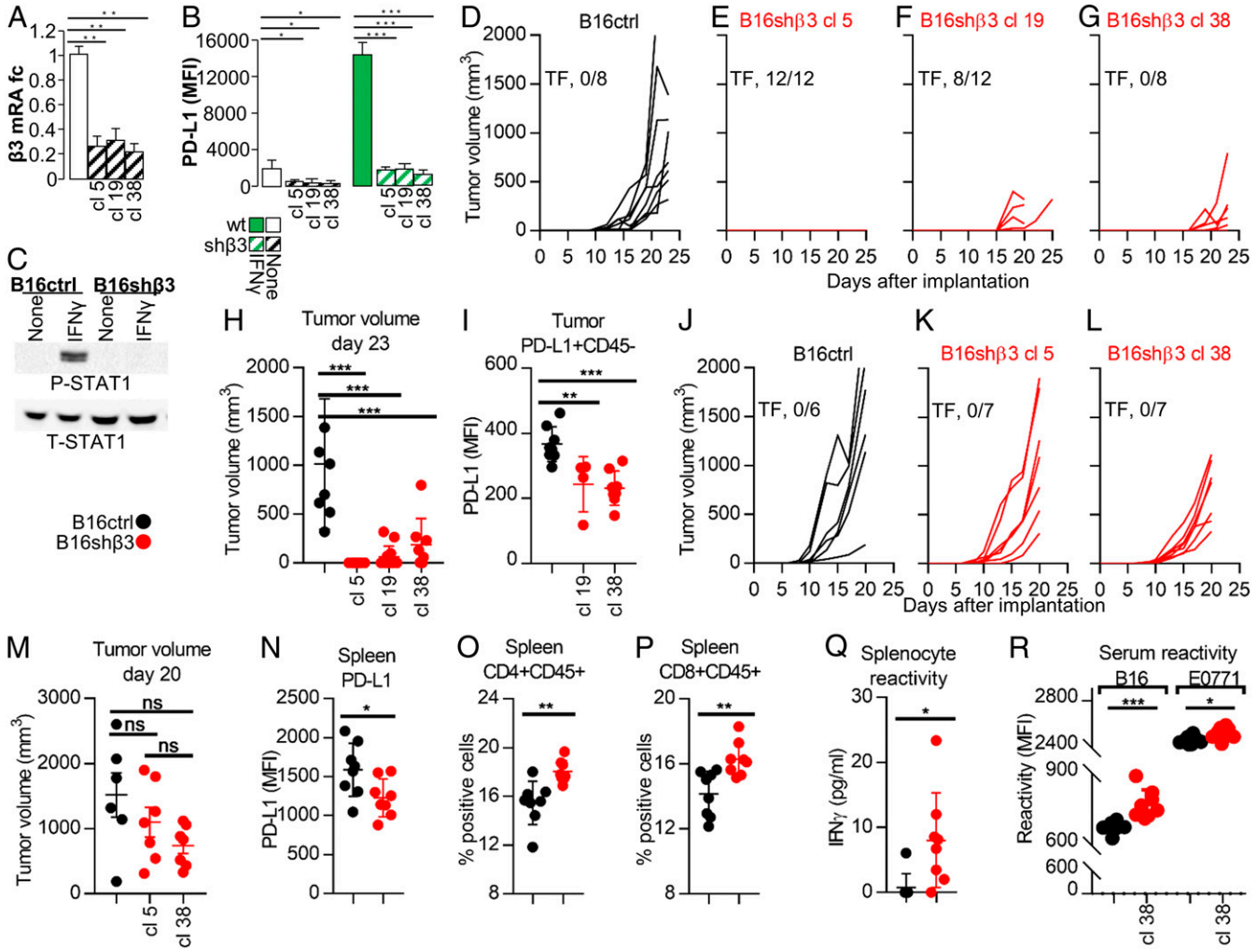

Fig. 4. B16 murine cancer cells stably depleted of β3-int (shβ3) exhibit reduced PD-L1 expression in vitro and in vivo and reduced tumor growth in vivo, and elicit a durable immune response. (*A*–*C*) Effect of stable β3-int depletion on PD-L1 expression and P-STAT1 in B16shβ3 or B16ctrl cells. (*A*) Extent of β3-int silencing in B16shβ3 (3 clones) measured as β3 mRNA levels. (*B*) Reduction of PD-L1 MFI in B16shβ3 clones, unexposed (no IFN) or exposed to IFNγ (100 IU) for 24 h. (*C*) P-STAT1 and T-STAT1 in B16ctrl or shβ3 cl 38 cells. Details are as in the legend to Fig. 1. (*D*–*R*) C57BL/6 and NOD-scid mice implanted with B16ctrl or B16shβ3 clones. (*D*–*G*) Growth kinetics of the primary tumor in C57BL/6 mice. TF, number of tumor-free/treated mice. (*H*) Tumor volume at day 23. (*I*) PD-L1 expression (MFI) in the CD45-negative tumor cells. (*J*–*L*) Growth kinetics of the primary tumor in NOD-scid mice. (*M*) Tumor volume in NOD-scid mice at day 20. (*N*–*R*) Characterization of spleens and sera of B16shβ3 cl 38-implanted C57BL/6 mice. Mice were killed at day 24. (*N*) PD-L1 MFI in splenocytes. (*O* and *P*) percentage of CD4+ (*O*) or CD8+ splenocytes (*P*). (*Q*) Splenocyte reactivity to WT B16 cells, quantified as IFNγ release. (*R*) Serum reactivity to WT B16 or EO771 cells, measured as MFI. In *A* and *B*, histograms represent the average of triplicates ±SD. *C* shows representative images of triplicate experiments. *D*–*I* represent data of C57BL/6 mice implanted with B16ctrl (8 mice) or B16shβ3 cl 5, 19, and 38 (12, 12, and 8 mice, respectively) cells. *N*–*R* represent data of B16ctrl (8 mice) or B16shβ3 cl 38 (8 mice). *J*–*L* represent data of NOD-scid mice implanted with B16ctrl (6 mice) or B16shβ3 cl 5 and 38 (7 and 7 mice, respectively) cells. Statistical significance was calculated by means of the *t* test (*N*–*R*) or 1-way ANOVA (*A*, *B*, *H*, *I*, and *M*). $*P < 0.05$, $**P < 0.01$, $***P < 0.001$; ns, nonsignificant.

Since PD-L1 is a master regulator of the immune response to tumors, we searched for markers indicative of a durable immune response. In the shβ3 arm the splenocyte PD-L1 was decreased (Fig. 4*N* and *SI Appendix*, Fig. S4*H*), and the CD4+ and CD8+ populations were increased (Fig. 4 *O* and *P* and *SI Appendix*, Fig. S4 *I* and *J*). Remarkably, the splenocyte reactivity to B16 cells (Fig. 4*Q*) and the serum reactivity to B16, but not to EO771 cell antigens were specifically increased (Fig. 4*R* and *SI Appendix*, Fig. S4 *K* and *L*). The latter data provide evidence that the depletion of β3-int in tumor cells elicits a distant immune response to B16 tumor cells.

B16 Cancer Cells Depleted of αvβ3-Int Elicit an Abscopal Immunotherapeutic Response. The above conclusion was strengthened in studies of B16 cells in which β3-int was transiently depleted (Fig. 5*A* and *SI Appendix*, Fig. S5 *A* and *B*). PD-L1 protein expression—both constitutive and IFNγ-inducible—was strongly diminished, especially early after small interfering (si)RNA transfection (Fig. 5*B* and *SI Appendix*, Fig. S5*C*). β3-int depletion also decreased IFNγ-induced P-STAT1 (Fig. 5*C*). When B16 cells transfected with siRNAβ3 or siRNActrl were implanted in C57BL/6 mice, primary tumor growth was almost completely abolished: 7/10 mice which received B16-siRNAβ3 (β3-depleted arm) were tumor-free versus 0/8 mice which received B16-siRNActrl (Fig. 5 *D* and *E*). In the 3 mice with tumors, the tumor specimens were too small for analysis. The finding that 3 independent clones and the siRNAβ3 cells behaved in a very similar manner with respect to the decrease in PD-L1 expression and tumor growth inhibition indicates that the observed phenotypes can be ascribed to β3-int depletion. The protected mice from the β3-depleted arm enabled us to ask whether β3-int–depleted tumors elicit an abscopal effect. Eighteen days after primary tumor implantation, the mice were challenged

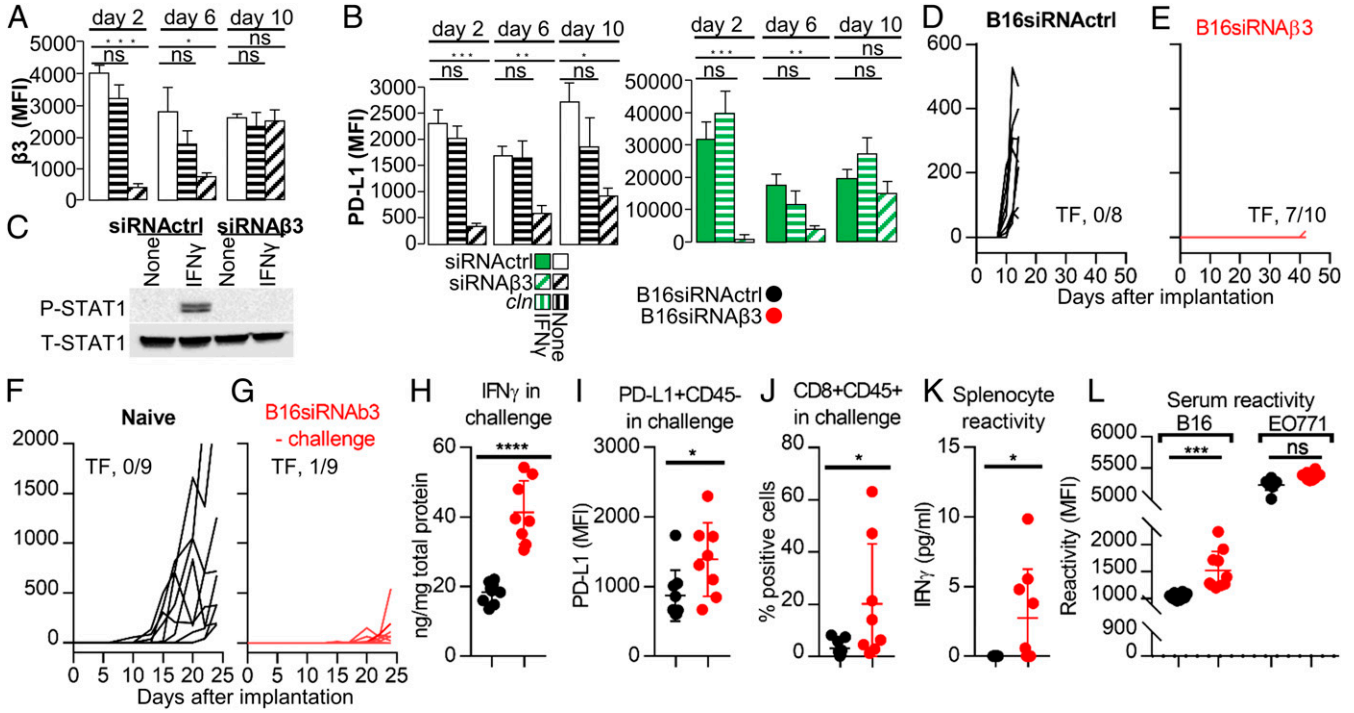

Fig. 5. B16 murine cancer cells transiently depleted of β3-int exhibit a reduction in PD-L1 expression in vitro and in the growth of primary and challenge tumors, and the challenge tumors show signs of immunotherapeutic effects. Long-term reactivity of splenocytes and serum. (*A–C*) Effect of transient β3-int depletion on PD-L1 and P-STAT1. B16 cells were transiently depleted of β3-int by siRNAβ3 (B16siRNAβ3), or mock-depleted by scrambled siRNA (B16siRNActrl), by siRNA transfection. (*A*) β3-int silencing (MFI) at day 2, 6, and 10 after siRNA transfection. (*B*) PD-L1 MFI in β3-int–depleted cells, unexposed (no IFN) or exposed to IFNγ (100 IU) for 24 h, and measured at day 2, 6, and 10. (*C*) P-STAT1 and T-STAT1 6 d after siRNA transfection. Details are as in the legend to Fig. 1. (*D–L*) C57BL/6 mice were implanted with B16siRNActrl (black) or B16siRNAβ3 (red) cells. (*D* and *E*) Growth kinetics of the primary tumor. (*F* and *G*) Mice previously implanted with B16siRNAβ3 cells (red) (*G*), at day 18 after primary tumor implantation, or naïve mice (black) (*F*) received a challenge tumor made of B16siRNActrl cells. Kinetics of the challenge tumor growth. (*H–L*) Characterization of the challenge tumor in the siRNAβ3 arm (red) or siRNActrl arm (black). (*H*) IFNγ content of tumors. (*I*) PD-L1 in CD45− tumor cells. (*J*) CD8+/CD45+ cells. (*K*) Splenocyte reactivity to B16 cells, quantified as IFNγ release. (*L*) Serum reactivity to B16 and unrelated EO771 cells. In *A* and *B*, histograms represent the average of triplicates ±SD. In *C* are representative images of repeated triplicate experiments. *D* and *E* represent data of B16siRNActrl (8 mice) or B16siRNAβ3 (10 mice) arms. *F–L* represent data of naïve (B16siRNActrl, 9 mice) or B16siRNAβ3 challenge (9 mice in *K* and *L*; 8 tumors in *G–J*). Statistical significance was calculated by *t* test (*H–L*) or 1-way ANOVA (*A* and *B*). $*P < 0.05$, $**P < 0.01$, $***P < 0.001$, $****P < 0.0001$; ns, nonsignificant.

in the contralateral flank with a tumor composed of B16 siRNActrl cells. The mice from the β3-int–depleted arm exhibited a strong reduction in the growth of the challenge tumor (Fig. 5*G*) relative to tumor growth in naïve mice (Fig. 5*F*). The explanted challenge tumors showed the presence of immune response. Thus, IFNγ and PD-L1 in the CD45-negative fraction—which included the tumor cells—were significantly increased in the β3-depleted arm (Fig. 5 *H* and *I* and *SI Appendix*, Fig. S5*D*). Tumor-infiltrating CD8+ lymphocytes were increased (Fig. 5*J* and *SI Appendix*, Fig. S5*E*). The derepression of the intratumoral immunosuppressive phenotype resulted in a systemic, durable immune response indicated by the increased splenocyte reactivity to B16 cells (Fig. 5*K*) and the increased serum reactivity to B16, but not the unrelated EO771, cell antigens (Fig. 5*L* and *SI Appendix*, Fig. S5 *F* and *G*). Cumulatively, these results show that the depletion of β3-int in murine cancer cells 1) results in a decrease in PD-L1 and a dramatic reduction in primary tumor growth, and 2) elicits a distant, durable immunotherapeutic response indicated by a reduction in challenge tumor growth, an increase in typical markers of immune activation—IFNγ and PD-L1—and CD8+ cell infiltration, and a durable, systemic immune response indicated by splenocyte and serum reactivity to tumor cell antigens.

αvβ3-Int Regulates PD-L1 Expression and Tumor Growth in 4T1 Breast Cancer Cells. We confirmed the role of αvβ3-int in tumor growth and immune response to tumors in the system of 4T1 breast cancer cells syngeneic with BALB/c mice. The cells were transiently depleted of β3-int by transfection of β3-siRNA. Control cells received siRNActrl. Fig. 6 *A* and *B* and *SI Appendix*, Fig. S6 *A* and *B* show the kinetics of silencing and the concomitant decrease in constitutive and IFNγ-induced PD-L1 expression, relative to WT-4T1 and siRNActrl cells. When implanted in BALB/c mice, the 4T1siRNAβ3 cells exhibited a strong reduction in tumor growth (Fig. 6 *C–F*) and a concomitant decrease in PD-L1 expression in the CD45-negative cell population (Fig. 6*G* and *SI Appendix*, Fig. S6*C*) and increase in IFNγ (Fig. 6*H*). Also in this model system the implantation of β3-int–depleted tumor cells resulted in a durable immune response, indicated by the increase in CD4+ and CD8+ splenocytes (Fig. 6 *I* and *J* and *SI Appendix*, Fig. S6 *D* and *E*), by splenocyte reactivity to 4T1 cells (Fig. 6*K*), and, furthermore, by the serum reactivity to 4T1 but not to unrelated B16 cells (Fig. 6*L* and *SI Appendix*, Fig. S6 *F* and *G*).

β3-Integrin Depletion Primes for Efficacy of Checkpoint Blockade. Finally, we investigated the effect of the combination of β3-int depletion with CP blockade. We chose to use stably depleted clone 38 cells because they gave rise to measurable tumors. We scored tumor formation for longer than the time indicated in Fig. 4. C57BL/6 mice were implanted with control or shβ3 cl 38 B16 cells and treated intraperitoneally (i.p.) with anti–PD-1 or control Abs 7, 12, 18, and 24 d after tumor implantation (see Fig. 7*A* for a schematic view of the experimental design). All mice that received one of the monotreatments exhibited a significant, temporary reduction and delay in tumor growth (Fig. 7 *B–D* and *F*).

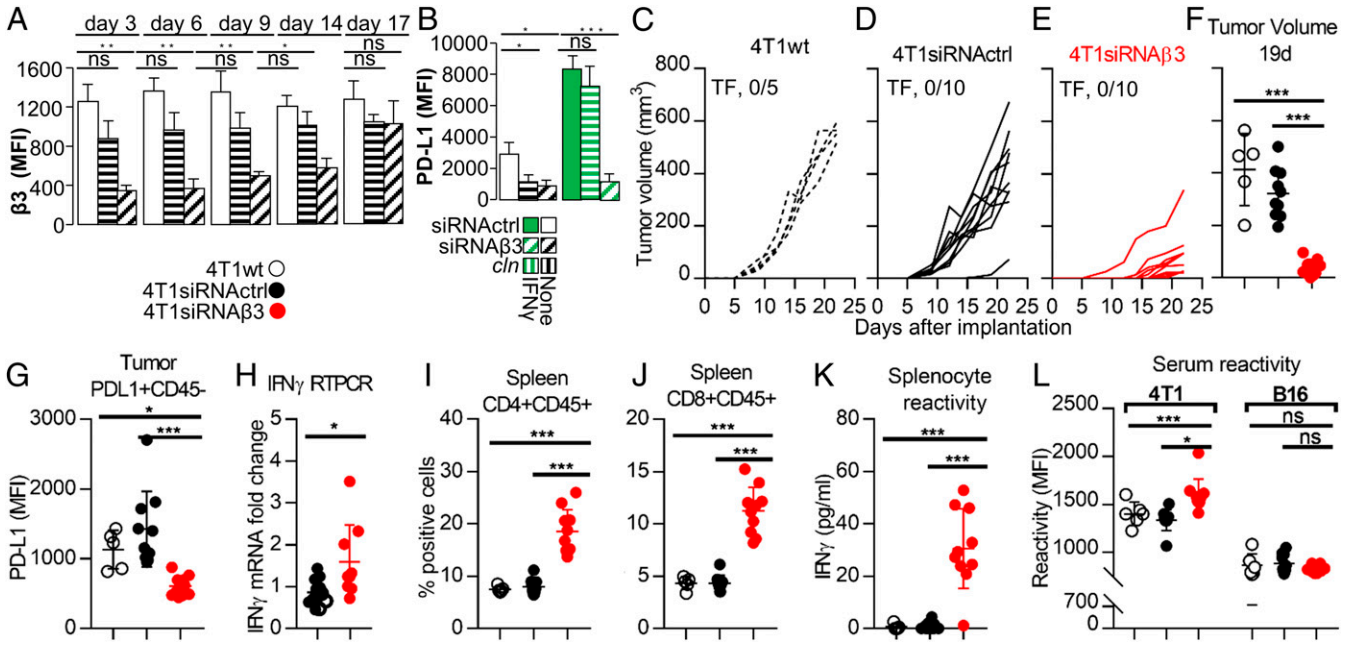

Fig. 6. 4T1 murine cancer cells transiently depleted of β3-int exhibit a reduction in PD-L1 expression in vitro and in the growth of the primary tumor. Long-term reactivity of splenocytes and serum. (*A* and *B*) Effect of transient β3-int depletion on PD-L1 expression. 4T1 cells were transiently depleted of β3-int by siRNAβ3 (4T1siRNAβ3), or mock-depleted by scrambled siRNA control (4T1siRNActrl), by siRNA transfection. (*A*) Extent of silencing measured by flow cytometry at 3, 6, 9, 14, and 17 d after siRNA transfection. (*B*) Reduction in PD-L1 expression in β3-int–depleted cells. 4T1WT, 4T1siRNActrl, or 4T1siRNAβ3 cells were unexposed (no IFN) or exposed to IFNγ (100 IU) for 24 h. (*C*–*L*) BALB/c mice were implanted with 4T1WT (black dashed lines) (*C*), 4T1siRNActrl cells (black) (*D*), or 4T1siRNAβ3 (red) cells (*E*). (*F*) Tumor volume at day 19 after primary tumor implantation. (*G*) PD-L1 in tumor cells (intratumoral CD45− cells). (*H*) IFNγ expression in tumors. (*I* and *J*) CD4+/CD45+ and CD8+/CD45+ cell populations in spleen. (*K*) Splenocyte reactivity to 4T1 cells, quantified as IFNγ release. (*L*) Serum reactivity to 4T1 and to the unrelated B16 tumor cells. In *A* and *B*, histograms represent the average of triplicates ±SD. *C*–*G* and *I*–*L* represent data of 4T1WT (5 mice), 4T1siRNActrl (10 mice), or 4T1siRNAβ3 (10 mice) arms. *H* represents data of 4T1WT (4 mice), 4T1siRNActrl (7 mice), or 4T1siRNAβ3 (8 mice) arms. Statistical significance was calculated by means of the *t* test (*H*) or 1-way ANOVA (*A*, *B*, *F*, *G*, and *I*–*L*). $*P < 0.05$, $**P < 0.01$, $***P < 0.001$; ns, nonsignificant.

However, none of the mice were tumor-free, and they all ultimately died because of their primary tumor. In the combination arm (β3-int–depleted tumor + anti–PD-1 Abs), there was a further reduction/delay (Fig. 7 *E*–*G*); 3/8 mice were free of primary tumors, and 2 carried small tumors (<400 mm^3). After 26 d, the mice in the combination group ($n = 7$) received a contralateral challenge tumor composed of WT cells (5 engrafted/7). After 55 d, the tumor-positive mice (challenge tumor alone, $n = 1$; primary and challenge tumors, $n = 3$) were killed, and the 2 mice free of both primary and challenge tumors were designated as long survivors (Fig. 7*A*). Altogether, the combination treatment resulted in very high protection; only 2/8 mice were dead at day 40, whereas all mice from the other 3 groups were dead. The Kaplan–Meier survival curve highlighted the highly statistically significant advantages of β3-int depletion (compare shβ3 with ctrl cells) and the additive effect of combination treatment (compare shβ3 with no Ab to shβ3 with anti–PD-1) (Fig. 7*H*). To gain mechanistic insight into this protection, we analyzed tumor specimens. The samples from the mice that received the combination treatment exhibited significant infiltration of CD8+ cells (Fig. 7*I* and *SI Appendix*, Fig. S7*A*). This feature suggested the reversal of the immunosuppressive phenotype. Accordingly, in depleted tumors, IFNγ and PD-L1 in the CD45+ lymphocyte fraction were increased (Fig. 7 *J* and *K* and *SI Appendix*, Fig. S7*B*), whereas PD-L1 in the CD45− fraction, which included the tumor cells, decreased (Fig. 7*L* and *SI Appendix*, Fig. S7*C*), further confirming that, even in vivo, β3-int depletion resulted in decreased PD-L1 expression in the tumor cells. Of note, the 2 findings that β3-int depletion resulted in the decrease in PD-L1 in vitro and in vivo and that inhibition of the PD-1/PD-L1 axis by anti–PD-1 antibodies (Fig. 7*F*) resulted in tumor growth inhibition strongly argue that the decrease in tumor growth induced by β3-int depletion can be ascribed, at least in part, to its effect on PD-L1 expression. This conclusion is reinforced by the observation that both treatments—β3-int depletion or anti–PD-1 MAb therapy—induced similar changes in the tumor microenvironment, namely an infiltration of CD8+ cells and increase in IFNγ.

The reversal of the immunosuppressive phenotype resulted in a durable immune response and abscopal protection. This was documented by the dramatic decrease in challenge tumor growth, or the absence of the challenge tumors relative to tumors in naïve mice (Fig. 7*M*), by CD8+ cell infiltration in the challenge tumors (Fig. 7*I*), and by the presence of B16 cell antibodies in sera at sacrifice (Fig. 7*N* and *SI Appendix*, Fig. S7*D*). Specifically, the antibody reactivity was high in mice that received the depleted tumor cells, even higher in those that received combination treatment, and highest in the long survivors (Fig. 7*N*). We conclude that the unleashing of the immunosuppressive microenvironment by β3-int depletion primed cells for anti–PD-1 therapy. Combination treatment induced strong immunotherapeutic and durable abscopal effects.

Discussion

Integrins are multifunctional cell-surface constituents of noncancerous and cancerous cells, which regulate several key functions, including the cell cycle and growth (14–16). Abundantly expressed in tumor cells and in cells of the tumor microenvironment, they contribute to tumor growth, acquisition of a metastatic phenotype, and stemness (18–20). αvβ3-int in endothelial cells contributes to neoangiogenesis (15, 21).

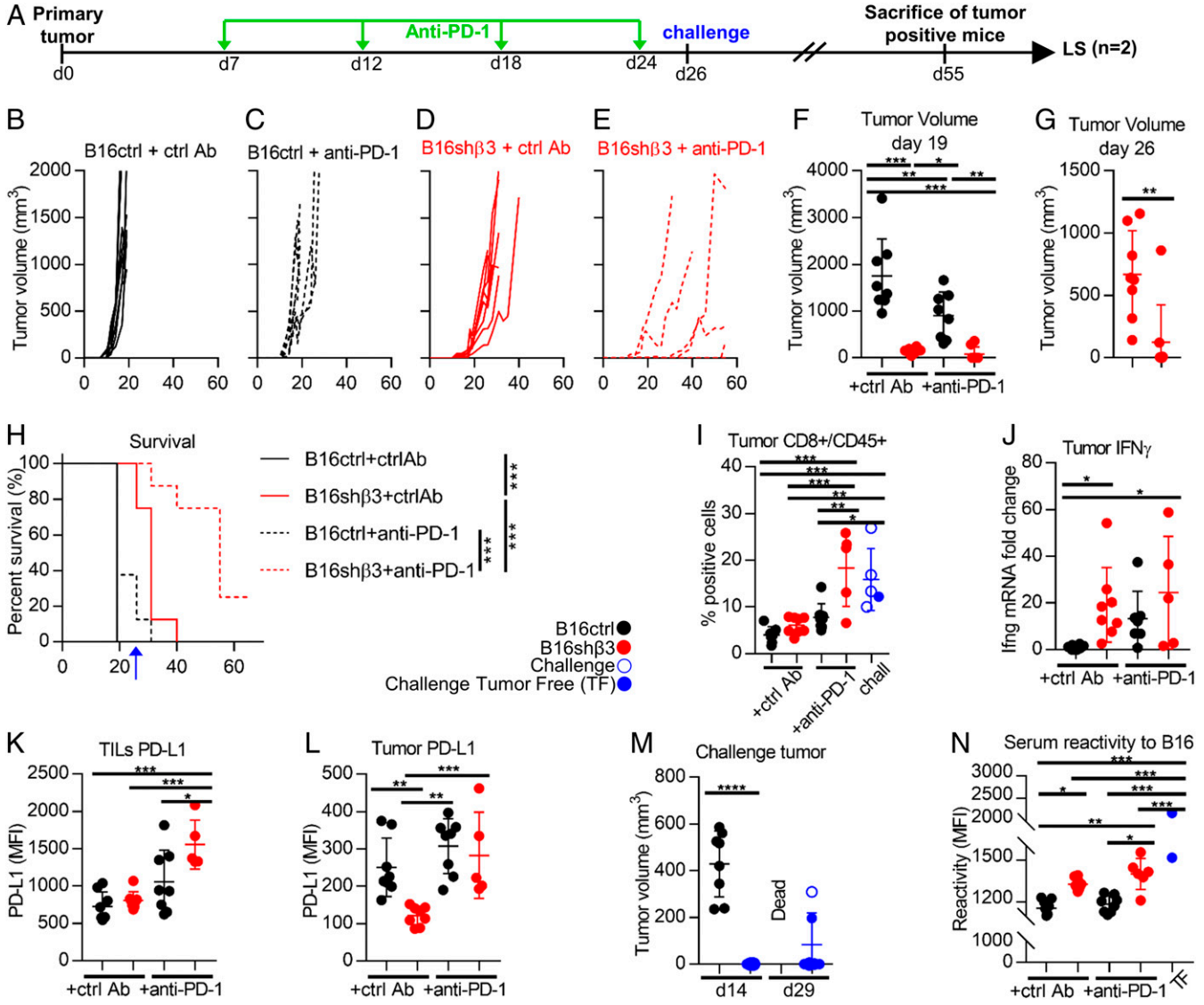

Fig. 7. Combination of β3-int depletion and anti–PD-1 therapy elicits an immunotherapeutic abscopal effect. (*A*) Schematic drawing of the experimental design. Green arrows indicate anti–PD-1 or control Ab administration. (*B–G*) C57BL/6 mice were implanted with B16ctrl (black) (*B* and *C*) or B16shβ3 (red) (*D* and *E*) cells. (*C* and *E*) At day 6, 12, 18, and 24, mice received i.p. injections of anti–PD-1 Abs (200 μg per mouse). (*B–E*) Kinetics of tumor growth. (*F* and *G*) Tumor volumes at day 19, when all mice were still alive, and at day 26, when only the mice implanted with shβ3 cells were alive. (*H*) Kaplan–Meier survival curve. The blue arrow indicates the time of challenge tumor implantation. (*I–N*) Characterization of primary and challenge tumors. Challenge tumors (blue) in the B16shβ3 + anti–PD-1 arm, with mice positive (empty dots) or negative (full dots) for the primary tumor. (*I*) CD8+/CD45+ cells in tumors from the indicated groups. (*J*) Relative intratumoral IFNγ mRNA levels, determined by qRT-PCR. (*K* and *L*) PD-L1 MFI in intratumoral CD45+ (*K*) and CD45− cells (*L*). (*M*) Challenge tumor volumes at the indicated days after its implantation. (*N*) Serum Ab reactivity to WT-B16 cells. *B–N* represent data of B16ctrl + ctrl Ab (8 mice), B16ctrl + anti–PD-1 (8 mice), B16shβ + ctrl Ab (8 mice), and B16shβ3 + anti–PD-1 (8 mice, but only 5 tumors in *I–N*). Statistical significance was calculated by the *t* test (*G* and *M*), 1-way ANOVA (*F*, *I–L*, and *N*), or log-rank test (Mantel–Cox) (*H*). $*P < 0.05$, $**P < 0.01$, $***P < 0.001$, $****P < 0.0001$.

We report that αvβ3-int regulates IFNα/βR and IFNγR signaling and PD-L1 expression in human and murine cancerous and noncancerous cells in vitro and in vivo, and thus is involved in tumor immune evasion (Fig. 8). The evidence for these conclusions includes the following.

Inducible PD-L1 expression was regulated by αvβ3-int upon exposure to IFNγ, IFNα, and IFNβ. This regulation took place in human cancerous and noncancerous cells. Specifically, αvβ3-int depletion or blockade dramatically decreased PD-L1 expression and STAT1 phosphorylation. Of the other IFN-sensitive genes tested, IRF7, like PD-L1, was positively regulated by αvβ3-int, whereas SOCS1 was negatively regulated. The αvβ3-int–mediated regulation of PD-L1 expression via IFNR signaling is consistent with the finding that resistance to anti–PD-1/PD-L1 therapy, among others, maps to the IFNR pathway (12, 13). Previous reports highlighted the cooperation of αvβ3-int and monocyte integrins with IFN signaling (36–38). The current findings center on αvβ3-int as a key player in the regulation of PD-L1 expression and tumor immune evasion.

αvβ3-int also regulated the constitutive expression of PD-L1, which likely took place independent of IFNR signaling through molecules usually regulated by αvβ3-int, such as PI3K/AKT, the MAPK cascade, CBL (Casitas B-lineage lymphoma), and NF-κB (39–42). We speculate that their documented involvement in the regulation of PD-L1 expression and antitumor immunity evasion (6, 43, 44) may depend on the fact that they are downstream targets of the αvβ3-int axis. This would provide a unifying mechanism for this set of proteins that regulate integrin-dependent constitutive and inducible PD-L1 expression.

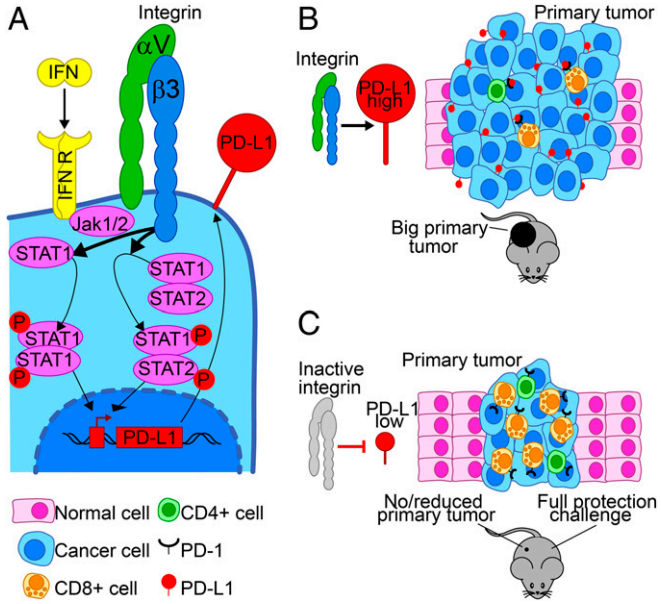

Fig. 8. Schematic view of the role of αvβ3-int in PD-L1 expression and antitumor immunity. αvβ3-int regulates PD-L1 expression through the IFNR pathway (*A*) and affects local and systemic antitumor immunity (*B*). The depletion of αvβ3-int or its block decreases the IFN-induced STAT1 phosphorylation. This regulation occurs through the β3 C tail. In β3-int–depleted cells, the reduced P-STAT1 negatively regulates IFN-stimulated gene transcription and results in low PD-L1 expression. αvβ3-int block negatively regulates PD-L1 also in murine tumor cells, in vitro and in vivo. Integrin inhibition in cancer cells results in local PD-L1 decrease and in the reduction in the primary tumor growth (*C*). Integrin inhibition in the primary tumor elicits an abscopal immunotherapeutic effect, resulting in the protection from a challenge tumor (*C*). Hallmarks of this acquired protection in the challenge tumor are highly reduced tumor growth, an increase in CD4+ and CD8+ lymphocyte infiltration, and high intratumoral IFNγ. The acquired systemic anti-B16 cell immunity is indicated by splenocytes' memory reactivity against B16 cells and by serum antibodies to B16 cells.

At the mechanistic level, αvβ3-int affected IFNR signaling through its β3 C tail, particularly residues Y747 and Y759, which are critical for integrin signaling. Interestingly, while we report that the regulation of PD-L1 expression in tumor cells was specifically mediated by αvβ3-int but not αvβ6- or αvβ8-integrin, Nishimura and colleagues recently reported that αvβ8-integrin on tumor cells contributed to tumor immune evasion by activating TGFβ in immune cells (33). Thus, different αv-integrins appear to play multiple, nonredundant roles in tumor immune evasion—some of which are PD-L1–dependent and some PD-L1–independent—and carry out this function by targeting different cell populations in the tumor bed.

The negative regulation of PD-L1 expression upon αvβ3-int depletion also occurred in murine tumor cells, in vitro and in vivo. The most striking in vivo effects were a dramatic reduction in primary tumor growth and an abscopal immunotherapeutic effect, which consisted of protection from a distant challenge tumor characterized by high IFNγ and CD4+ and CD8+ lymphocyte infiltration and by memory reactivity exhibited by splenocytes and serum antibodies to cancer cells. The reduction in primary tumor growth was likely a multifactorial effect, in which the immune dysregulation and PD-L1 variation played a major role. In support are the low reduction in depleted tumor growth seen in immunodeficient mice, the consistent reduction in cancer cell PD-L1 and tumor growth seen in 2 immunocompetent mouse models, and the observation that inhibition of the PD-1/PD-L1 axis by means of anti–PD-1 Abs induced similar qualitative effects as β3-int blockade/depletion, including an increase in tumor IFNγ and in infiltrating CD8+ lymphocytes, indicative of "immune heating" of the tumor itself (Fig. 7). Well-known effects of β3-int depletion/blockade other than immune dysregulation (19), for example on the cell cycle and proliferation, played but minor effects on tumor growth, at least in the analyzed model systems. The inhibition of primary tumor growth observed here was clearly independent of the proangiogenic effects of αvβ3-int expressed in endothelial cells. A decrease in the growth of B16 tumor cells depleted of β3-int was previously described, but the underlying mechanism was not elucidated (45). We conclude that αvβ3-int is a driver of the tumor immune evasion system.

Major restrictions to CP immunotherapy are that susceptibility is limited to some cancer types, only a fraction of patients respond, and resistance and severe adverse effects develop in responder patients (46–50). To improve CPI therapy, ongoing efforts aim to induce immune heating of the immunosuppressive tumor microenvironment, albeit at the cost of increasing PD-L1 expression, and to combine such treatments with CPIs (51). Taking into account that αvβ3-int blockade unleashed the PD-1/PD-L1 inhibitory axis, that combination treatment with anti–PD-1 resulted in a high rate of protection and durable immunotherapeutic effect, and that αvβ3-int inhibition within the tumor is feasible, for example by the use of integrin mimetics, including the approved *cln* and novel peptides under evaluation (22, 52), we suggest that αvβ3-int blockade might be part of a multipronged attack on the PD-1/PD-L1 axis. This would increase the probability of success for CP blockade and decrease adverse effects and resistance onset. A β3-int antagonist can conceivably be administered by means of a vector, such as one expressed within the tumor bed by an appropriately armed oncolytic virus that might also encode CPIs.

Materials and Methods

Cells. SK-OV-3, MDA-MB-453, SK-BR-3, 4T1, SK-N-SH, U251, HT29, B16, and EO771 cells were purchased from the American Type Culture Collection and cultured as detailed in *SI Appendix*. GBM23 cells were described (32). The derivation of shβ3 clones or siRNAβ3 cells was described and is detailed in *SI Appendix*. To generate SK-OV-3 cells expressing WT or mutant αvβ3-int, cells were transfected with plasmids encoding αv_{WT} plus either $\beta 3_{WT}$ or $\beta 3_{Y747F,Y759F}$, selected with G418 for 2 wk, and tested for integrin heterodimer expression before use.

Antibodies, Soluble Proteins, and Inhibitors. The detailed source of antibodies is listed in *SI Appendix*. Recombinant human IFNβ (8499-IF/CF), IFNγ (285-IF/CF), universal type I IFN (IFNα, 11200), murine IFNγ (485-MI/CF), and IFNβ (8234-MB/CF) were supplied by R&D Systems. Cyclic (L-arginyl-glycyl-L-α-aspartyl-D-phenylalanyl-*N*-methyl-L-valyl) peptide, which is named *cln*, was supplied by Chematek. The STAT1 inhibitor fludarabine and P-MEK1/2 inhibitor U0126 were purchased from Sigma-Aldrich and Selleckchem, respectively.

Western Blot. Electrophoresis and Western blot (WB) were performed as detailed (25).

Reverse Transcription and qRT-PCR. Reverse transcription and qRT-PCR are detailed in *SI Appendix*.

In Vivo Experiments. C57BL/6, BALB/c, and NOD-scid mice were obtained from The Jackson Laboratory, Charles River Laboratories, and Plaisant, respectively. Mice were bred in a facility at the Department of Veterinary Medical Sciences, University of Bologna. Animal experimentation was carried out at the Department of Veterinary Medical Sciences or at Plaisant. Details of the experimental design are provided in the figure legends and in *SI Appendix*.

Splenocyte and Serum Reactivity to B16, 4T1, and Control Cells. Splenocyte derivation, their reactivity to cancer cells, and serum reactivity were described (53) and are detailed in *SI Appendix*.

Intratumoral IFNγ and Spleen-Infiltrating Lymphocytes. Intratumoral IFNγ and spleen-infiltrating lymphocytes were quantified by flow cytometry, as detailed in *SI Appendix* (53).

Statistical Analysis. The results of statistical analyses are reported in the figure legends where applicable as follows: $*P < 0.05$, $**P < 0.01$, $***P < 0.001$, $****P < 0.0001$.

Ethics Statement. Animal experiments were performed according to European Directive 2010/63/UE and Italian Laws 116/92 and 26/2014. The experimental protocols were reviewed and approved by the University of Bologna Animal Care and Use Committee ("Comitato per il Benessere degli Animali"; COBA) and approved by the Italian Ministry of Health, Authorization 86/2017-PR (to A.Z.). For the experiment conducted in the Plaisant facility, Authorization 1/2018-PR was provided.

ACKNOWLEDGMENTS. This work was supported by European Research Council ADG Grant 340060 (to G.C.F.) and the Department of Experimental, Diagnostic and Specialty Medicine through the Pallotti legacy (T.G.). The funders had no role in the study design, data collection and analysis, decision to publish, or preparation of the manuscript.

1. Y. Ishida, Y. Agata, K. Shibahara, T. Honjo, Induced expression of PD-1, a novel member of the immunoglobulin gene superfamily, upon programmed cell death. *EMBO J.* **11**, 3887–3895 (1992).
2. D. S. Chen, I. Mellman, Elements of cancer immunity and the cancer-immune set point. *Nature* **541**, 321–330 (2017).
3. A. H. Sharpe, E. J. Wherry, R. Ahmed, G. J. Freeman, The function of programmed cell death 1 and its ligands in regulating autoimmunity and infection. *Nat. Immunol.* **8**, 239–245 (2007).
4. P. Loke, J. P. Allison, PD-L1 and PD-L2 are differentially regulated by Th1 and Th2 cells. *Proc. Natl. Acad. Sci. U.S.A.* **100**, 5336–5341 (2003).
5. H. Dong *et al.*, Tumor-associated B7-H1 promotes T-cell apoptosis: A potential mechanism of immune evasion. *Nat. Med.* **8**, 793–800 (2002).
6. J. Chen, C. C. Jiang, L. Jin, X. D. Zhang, Regulation of PD-L1: A novel role of pro-survival signalling in cancer. *Ann. Oncol.* **27**, 409–416 (2016).
7. M. E. Keir, M. J. Butte, G. J. Freeman, A. H. Sharpe, PD-1 and its ligands in tolerance and immunity. *Annu. Rev. Immunol.* **26**, 677–704 (2008).
8. E. J. Beswick *et al.*, TLR4 activation enhances the PD-L1-mediated tolerogenic capacity of colonic CD90+ stromal cells. *J. Immunol.* **193**, 2218–2229 (2014).
9. J. Hamanishi *et al.*, Programmed cell death 1 ligand 1 and tumor-infiltrating CD8+ T lymphocytes are prognostic factors of human ovarian cancer. *Proc. Natl. Acad. Sci. U.S.A.* **104**, 3360–3365 (2007).
10. Q. Gao *et al.*, Overexpression of PD-L1 significantly associates with tumor aggressiveness and postoperative recurrence in human hepatocellular carcinoma. *Clin. Cancer Res.* **15**, 971–979 (2009).
11. R. S. Herbst *et al.*, Predictive correlates of response to the anti-PD-L1 antibody MPDL3280A in cancer patients. *Nature* **515**, 563–567 (2014).
12. J. M. Zaretsky *et al.*, Mutations associated with acquired resistance to PD-1 blockade in melanoma. *N. Engl. J. Med.* **375**, 819–829 (2016).
13. D. S. Shin *et al.*, Primary resistance to PD-1 blockade mediated by JAK1/2 mutations. *Cancer Discov.* **7**, 188–201 (2017).
14. R. O. Hynes, Integrins: Bidirectional, allosteric signaling machines. *Cell* **110**, 673–687 (2002).
15. J. S. Desgrosellier, D. A. Cheresh, Integrins in cancer: Biological implications and therapeutic opportunities. *Nat. Rev. Cancer* **10**, 9–22 (2010).
16. E. H. Danen, A. Sonnenberg, Integrins in regulation of tissue development and function. *J. Pathol.* **201**, 632–641 (2003).
17. Y. Kikkawa, N. Sanzen, H. Fujiwara, A. Sonnenberg, K. Sekiguchi, Integrin binding specificity of laminin-10/11: Laminin-10/11 are recognized by alpha 3 beta 1, alpha 6 beta 1 and alpha 6 beta 4 integrins. *J. Cell Sci.* **113**, 869–876 (2000).
18. W. Guo, F. G. Giancotti, Integrin signalling during tumour progression. *Nat. Rev. Mol. Cell Biol.* **5**, 816–826 (2004).
19. L. Seguin, J. S. Desgrosellier, S. M. Weis, D. A. Cheresh, Integrins and cancer: Regulators of cancer stemness, metastasis, and drug resistance. *Trends Cell Biol.* **25**, 234–240 (2015).
20. H. Hamidi, J. Ivaska, Every step of the way: Integrins in cancer progression and metastasis. *Nat. Rev. Cancer* **18**, 533–548 (2018).
21. F. Demircioglu, K. Hodivala-Dilke, αvβ3 integrin and tumour blood vessels—Learning from the past to shape the future. *Curr. Opin. Cell Biol.* **42**, 121–127 (2016).
22. M. Nieberler *et al.*, Exploring the role of RGD-recognizing integrins in cancer. *Cancers* **9**, E116 (2017).
23. H. M. Shepard, C. M. Brdlik, H. Schreiber, Signal integration: A framework for understanding the efficacy of therapeutics targeting the human EGFR family. *J. Clin. Invest.* **118**, 3574–3581 (2008).
24. J. M. Ricono *et al.*, Specific cross-talk between epidermal growth factor receptor and integrin alphavbeta5 promotes carcinoma cell invasion and metastasis. *Cancer Res.* **69**, 1383–1391 (2009).
25. T. Gianni, V. Leoni, L. S. Chesnokova, L. M. Hutt-Fletcher, G. Campadelli-Fiume, αvβ3-integrin is a major sensor and activator of innate immunity to herpes simplex virus-1. *Proc. Natl. Acad. Sci. U.S.A.* **109**, 19792–19797 (2012).
26. T. Gianni, G. Campadelli-Fiume, The epithelial αvβ3-integrin boosts the MYD88-dependent TLR2 signaling in response to viral and bacterial components. *PLoS Pathog.* **10**, e1004477 (2014).
27. T. Gianni, V. Leoni, G. Campadelli-Fiume, Type I interferon and NF-κB activation elicited by herpes simplex virus gH/gL via αvβ3 integrin in epithelial and neuronal cell lines. *J. Virol.* **87**, 13911–13916 (2013).
28. L. Seguin *et al.*, An integrin β_3-KRAS-RalB complex drives tumour stemness and resistance to EGFR inhibition. *Nat. Cell Biol.* **16**, 457–468 (2014).
29. K. Seystahl, D. Gramatzki, P. Roth, M. Weller, Pharmacotherapies for the treatment of glioblastoma—Current evidence and perspectives. *Expert Opin. Pharmacother.* **17**, 1259–1270 (2016).
30. M. David *et al.*, Requirement for MAP kinase (ERK2) activity in interferon alpha- and interferon beta-stimulated gene expression through STAT proteins. *Science* **269**, 1721–1723 (1995).
31. A. Garcia-Diaz *et al.*, Interferon receptor signaling pathways regulating PD-L1 and PD-L2 expression. *Cell Rep.* **19**, 1189–1201 (2017).
32. E. Carra *et al.*, Sorafenib selectively depletes human glioblastoma tumor-initiating cells from primary cultures. *Cell Cycle* **12**, 491–500 (2013).
33. N. Takasaka *et al.*, Integrin αvβ8-expressing tumor cells evade host immunity by regulating TGF-β activation in immune cells. *JCI Insight* **3**, 122591 (2018).
34. D. A. Reardon, L. B. Nabors, R. Stupp, T. Mikkelsen, Cilengitide: An integrin-targeting arginine-glycine-aspartic acid peptide with promising activity for glioblastoma multiforme. *Expert Opin. Investig. Drugs* **17**, 1225–1235 (2008).
35. R. A. Porritt, P. J. Hertzog, Dynamic control of type I IFN signalling by an integrated network of negative regulators. *Trends Immunol.* **36**, 150–160 (2015).
36. J. B. McCarthy, B. V. Vachhani, S. M. Wahl, D. S. Finbloom, G. M. Feldman, Human monocyte binding to fibronectin enhances IFN-gamma-induced early signaling events. *J. Immunol.* **159**, 2424–2430 (1997).
37. J. Ivaska, L. Bosca, P. J. Parker, PKCepsilon is a permissive link in integrin-dependent IFN-gamma signalling that facilitates JAK phosphorylation of STAT1. *Nat. Cell Biol.* **5**, 363–369 (2003).
38. T. Umemoto *et al.*, Integrin αvβ3 enhances the suppressive effect of interferon-γ on hematopoietic stem cells. *EMBO J.* **36**, 2390–2403 (2017).
39. F. Mainiero *et al.*, The coupling of alpha6beta4 integrin to Ras-MAP kinase pathways mediated by Shc controls keratinocyte proliferation. *EMBO J.* **16**, 2365–2375 (1997).
40. R. E. Bachelder *et al.*, p53 inhibits alpha 6 beta 4 integrin survival signaling by promoting the caspase 3-dependent cleavage of AKT/PKB. *J. Cell Biol.* **147**, 1063–1072 (1999).
41. K. Gowrishankar *et al.*, Inducible but not constitutive expression of PD-L1 in human melanoma cells is dependent on activation of NF-κB. *PLoS One* **10**, e0123410 (2015).
42. L. M. Shaw, I. Rabinovitz, H. H. Wang, A. Toker, A. M. Mercurio, Activation of phosphoinositide 3-OH kinase by the alpha6beta4 integrin promotes carcinoma invasion. *Cell* **91**, 949–960 (1997).
43. P. Ritprajak, M. Azuma, Intrinsic and extrinsic control of expression of the immunoregulatory molecule PD-L1 in epithelial cells and squamous cell carcinoma. *Oral Oncol.* **51**, 221–228 (2015).
44. A. Serrels *et al.*, Nuclear FAK controls chemokine transcription, Tregs, and evasion of anti-tumor immunity. *Cell* **163**, 160–173 (2015).
45. A. Nasulewicz-Goldeman, B. Uszczyńska, K. Szczaurska-Nowak, J. Wietrzyk, siRNA-mediated silencing of integrin β3 expression inhibits the metastatic potential of B16 melanoma cells. *Oncol. Rep.* **28**, 1567–1573 (2012).
46. N. P. Restifo, M. J. Smyth, A. Snyder, Acquired resistance to immunotherapy and future challenges. *Nat. Rev. Cancer* **16**, 121–126 (2016).
47. D. M. Pardoll, The blockade of immune checkpoints in cancer immunotherapy. *Nat. Rev. Cancer* **12**, 252–264 (2012).
48. W. Zou, J. D. Wolchok, L. Chen, PD-L1 (B7-H1) and PD-1 pathway blockade for cancer therapy: Mechanisms, response biomarkers, and combinations. *Sci. Transl. Med.* **8**, 328rv4 (2016).
49. P. Sharma, J. P. Allison, The future of immune checkpoint therapy. *Science* **348**, 56–61 (2015).
50. D. Liu, R. W. Jenkins, R. J. Sullivan, Mechanisms of resistance to immune checkpoint blockade. *Am. J. Clin. Dermatol.* **20**, 41–54 (2019).
51. A. Ribas *et al.*, Oncolytic virotherapy promotes intratumoral T cell infiltration and improves anti-PD-1 immunotherapy. *Cell* **170**, 1109–1119.e10 (2017).
52. J. F. Van Agthoven *et al.*, Structural basis for pure antagonism of integrin αVβ3 by a high-affinity form of fibronectin. *Nat. Struct. Mol. Biol.* **21**, 383–388 (2014).
53. V. Leoni *et al.*, A fully-virulent retargeted oncolytic HSV armed with IL-12 elicits local immunity and vaccine therapy towards distant tumors. *PLoS Pathog.* **14**, e1007209 (2018).

Correction

MICROBIOLOGY

Correction for "αvβ3-integrin regulates PD-L1 expression and is involved in cancer immune evasion," by Andrea Vannini, Valerio Leoni, Catia Barboni, Mara Sanapo, Anna Zaghini, Paolo Malatesta, Gabriella Campadelli-Fiume, and Tatiana Gianni, which was first published September 16, 2019; 10.1073/pnas.1901931116 (*Proc. Natl. Acad. Sci. U.S.A.* **116**, 20141–20150).

The authors note that an additional affiliation should be listed for Paolo Malatesta. The new affiliation should appear as Ospedale Policlinico San Martino, Istituto di Ricovero e Cura a Carattere Scientifico (IRCCS), 16132 Genova, Italy. The corrected author and affiliation lines appear below. The online version has been corrected.

Andrea Vannini[a], Valerio Leoni[a], Catia Barboni[b], Mara Sanapo[b], Anna Zaghini[b], Paolo Malatesta[c,d], Gabriella Campadelli-Fiume[a,1], and Tatiana Gianni[a]

[a]Department of Experimental, Diagnostic and Specialty Medicine, University of Bologna, 40126 Bologna, Italy; [b]Department of Veterinary Medical Sciences, University of Bologna, 40064 Bologna, Italy; [c]Department of Experimental Medicine, University of Genova, 16132 Genova, Italy; and [d]Ospedale Policlinico San Martino, Istituto di Ricovero e Cura a Carattere Scientifico (IRCCS), 16132 Genova, Italy

First published October 14, 2019.

www.pnas.org/cgi/doi/10.1073/pnas.1916790116